

# WEC Development Project

Winter Semester 2024/2025

## Final Design Report



Project Name: **Optimus Shakti 5.0**  
Sub-Project: **Turbine Controller**

**Prepared by:**      **Matriculation number:**

Felix Lehmann	670183
Karan Soni	760153
Julius Preuschoff	750203

**Supervisor**

David Schlipf

Date: January 3, 2025

# Contents

<b>List of Figures</b>	<b>iv</b>
<b>1 Introduction and motivation (Soni)</b>	<b>1</b>
<b>2 Controller design objectives</b>	<b>2</b>
2.1 Advanced Controller (Soni) . . . . .	2
2.2 Control Regions (Soni) . . . . .	2
2.3 Advanced Generator Torque controller (Soni) . . . . .	4
2.4 Collective Pitch Controller (CPC) (Julius) . . . . .	5
2.5 Tower Damper (Felix) . . . . .	6
<b>3 Further Things</b>	<b>11</b>
3.1 Wind Field Generation (Felix) . . . . .	11
3.2 Simple Storage System Dummy (Julius) . . . . .	12
3.2.1 Description . . . . .	12
3.2.2 Scenarios . . . . .	13
3.3 Tower Bending Stiffness (Julius) . . . . .	13
<b>4 Controller tuning</b>	<b>15</b>
4.1 Steady States (Soni) . . . . .	15
4.2 DEL calculations and Parameter Optimization (Felix) . . . . .	16
4.3 Minimum Pitch Angle Optimization (Julius) . . . . .	16
4.4 Minimum Pitch Angle Optimization for Control Region 1.5 (Julius) . . . . .	16
<b>5 Challenges, Teamwork and Lessons Learned</b>	<b>19</b>
5.1 Rated Wind Speed (Julius) . . . . .	19
5.2 Generator Speed and Control Region 2.5 (Felix) . . . . .	20
5.3 Mismatch of SLOW and FAST Model (Julius) . . . . .	20
5.4 High Blade Mass and Generator Inertia (Julius) . . . . .	21
5.5 Lessons Learned (Julius) . . . . .	22
5.6 Team (Felix) . . . . .	22
<b>6 Summary (Felix)</b>	<b>23</b>
6.1 Conclusion . . . . .	23
6.2 Improvements and Future Workflow . . . . .	23
<b>7 Appendix</b>	<b>24</b>
7.1 Project Order (Julius) . . . . .	24

7.2	Control Parameter (Felix)	24
7.3	Steady States (Julius)	24
<b>References</b>		<b>25</b>

## List of Figures

Figure 2.1 Advance Wind Turbine Controller . . . . .	2
Figure 2.2 Wind turbine control regions . . . . .	3
Figure 2.3 Wind turbine control regions . . . . .	4
Figure 2.4 Tower Damper in Simulink model . . . . .	7
Figure 2.5 Bode plot of the Lag-Compensator . . . . .	7
Figure 2.6 Pole-Zero-Map of the Lag-Compensator . . . . .	8
Figure 2.7 Tower Damper Estimated Tower-Top-Speed . . . . .	9
Figure 2.8 Tower-Top-Speed . . . . .	10
Figure 2.9 Spectrum of the tower base bending moment . . . . .	10
Figure 3.1 Combined timeseries with Turbulence Class B . . . . .	12
Figure 3.2 Storage dummy in Simulink model . . . . .	13
Figure 3.3 Curtailment scenario for 4h duration, a storage capacity of 5 MWh and a curtailment rate of 6 %. . . . .	14
Figure 4.1 Power curve calculated with steady state calculations . . . . .	16
Figure 4.2 brute force optimization for minimum pitch angle $\theta$ . . . . .	17
Figure 4.3 brute force optimization for minimum pitch angle $\theta$ in region 1.5 . . . . .	18

## 1 Introduction and motivation (Soni)

The report provides an overview of the dynamic controller for the OPTIMUS-Shakti-5MW wind turbine. Developed as part of the "Development of a Wind Turbine" module in the Wind Energy Engineering Master's program at the University of Applied Sciences in Flensburg, this prototype aims to prepare students with the skills needed to develop a wind turbine. This year's OPTIMUS turbine has a rated power of 5MW and a rotor diameter of 178 meters. Based on the tubular concept with a gearbox drivetrain, it is planned for onshore installation in Karnataka.

General objectives and requirements regarding the design of a dynamic controller will be discussed in the following chapter. It is important to highlight the challenges posed by operating in low wind speed areas. One critical aspect is the large rotor disc, which must perform efficiently under these conditions. The varying wind speeds result in dynamic loads that the control system must manage.

For the design of the advanced controller, we used a 3.4 MW reference wind turbine from the IEA Wind TCP Task 37 as a benchmark. This provided a solid foundation for developing a reliable control system that optimizes performance under various conditions.

The report covers essential topics in wind turbine design and optimization, including wind generation, a simple storage system with scenarios, tower bending stiffness, and peak shaving. It also addresses controller tuning. Challenges faced, generator speed control in Region 2.5, rated wind speed, and the mismatch between SLOW and FAST models are discussed. The report concludes with a summary of milestones achieved and an evaluation of the dynamic controller's integration into the OPTIMUS-Shakti-5MW wind turbine system.

## 2 Controller design objectives

### 2.1 Advanced Controller (Soni)

Wind turbine use closed-loop control (maximum energy capture over normal operation and less structural load) systems to continuously adjust their operations based on feedback. Figure 1, illustrates the advanced closed-loop control diagram of a wind turbine.

The torque controller optimizes power production below rated speed and maintain rated power above rated wind speed by adjusting generator torque ( $M_G$ ) based on generator speed ( $\Omega_G$ ). Advance torque control uses a PI controller with anti-windup to regulate the generator torque based on the difference between the actual and reference generator speeds. Above rated wind speed, Pitch controller maintains the rated generator speed ( $\Omega_{G,rated}$ ) by adjusting blade pitch angle ( $\theta$ ), which ensures the rated power is maintained. With increasing wind speed, the pitch angle increases to reduce power coefficient ( $c_p$ ). Once the wind speed reaches the rated value, the generator torque is maintained at its rated value. The control is categorized into different regions, as detailed in Section 2.2.

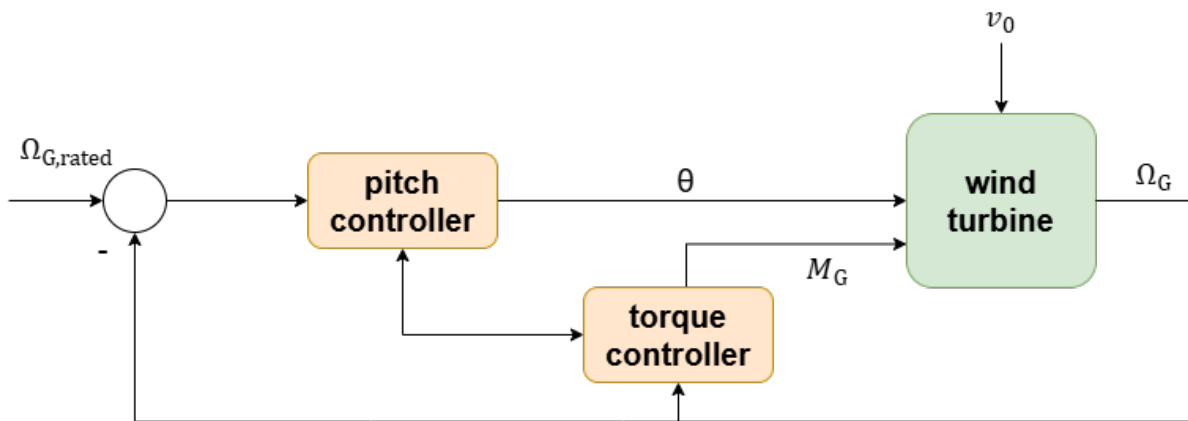


**Figure 2.1** Advance Wind Turbine Controller

### 2.2 Control Regions (Soni)

Wind turbine operations are segmented into three primary regions based on varying wind speed. These regions are defined by the turbine power output relative to wind speed. These regions are detailed below and illustrated in Figure 2.2.

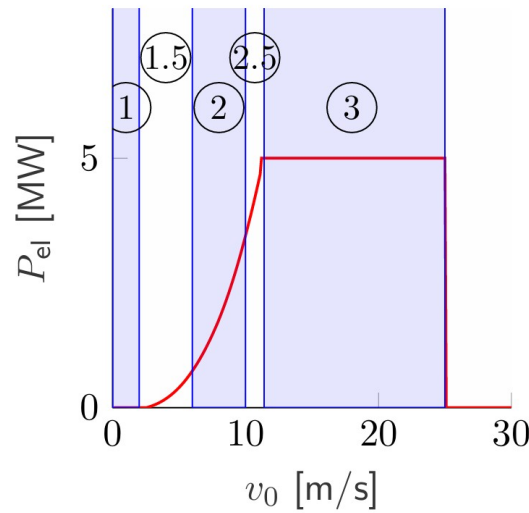


**Figure 2.2** Wind turbine control regions  
[4]

**Region 1:** When the wind speed is below the cut-in speed ( $v_{in}$ ), the turbine does not generate any power and remains stationary.

**Region 1.5:** This phase indicates the shift to Region 2, where wind speeds are sufficient to accelerate rotor. The generator torque is carefully controlled to accelerate the transition to Region 2. While energy production has started, the power output remains relatively low. The goal is to quickly reach Region 2, where the turbine can operate more efficiently.

**Region 2:** Wind speeds are above the cut-in speed ( $v_{in}$ ) but below the rated wind speed ( $v_{rated}$ ). The primary objective is to maximize energy yield. To achieve this, the turbine operator at the optimal power coefficient ( $c_{P,opt}$ ), which is determined by reaching the optimal tip speed ratio ( $\lambda_{opt}$ ) and pitch angle ( $\theta_{opt}$ ). The control system ensures that the turbine maintains these optimal conditions by regulating the rotational speed through the torque controller. In this region, the generator torque is adjusted based on rotor speed, as shown in Equation 2.1.

$$M_G = \frac{1}{2} \rho R^5 \frac{P_{opt}}{\lambda_{opt}^3 r_{GB}^3} \Omega_G^2 \quad (2.1)$$

$$M_G = k \Omega_G^2 \quad (2.2)$$

**Region 2.5:** This phase represents a transition between Region 2 and Region 3. In this region, the wind speed is increasing, and the turbine is approaching its rated wind speed. The control system continues to optimize the generator torque to ensure a smooth transition. Energy production is higher compared to Region 2, but the turbine has not yet reached its maximum power output. The pitch controller begins to act to keep the thrust on the rotor as low as possible while aiming to reach the rated speed as quickly as possible.

**Region 3:** In this region, wind speeds have reached the rated wind speed, and the primary goal is to generate maximum power. The control goal is maintain rated power and generator speed as well as reduce structure loads. The torque controller maintains the generator torque at its rated value. The pitch controller actively adjusts the blade pitch angle to regulate the power and keep it within the turbine rated capacity.

## 2.3 Advanced Generator Torque controller (Soni)

Generator torque is one of the two main control inputs for a wind turbine. The performance of an advanced generator torque controller offers significant improvements and greater flexibility compared to a baseline torque controller. The primary goals of the advanced torque controller are to reach the optimal power curve earlier and to maintain it for a longer duration compared to the baseline controller. Additionally, the dynamics in Regions 1.5 and 2.5 are tunable, allowing for more precise control.

Goals of the advanced torque controller:

- Achieve the optimal power curve earlier.
- Maintain the optimal power curve for a longer period.
- Enable tunable dynamics in Regions 1.5 and 2.5.

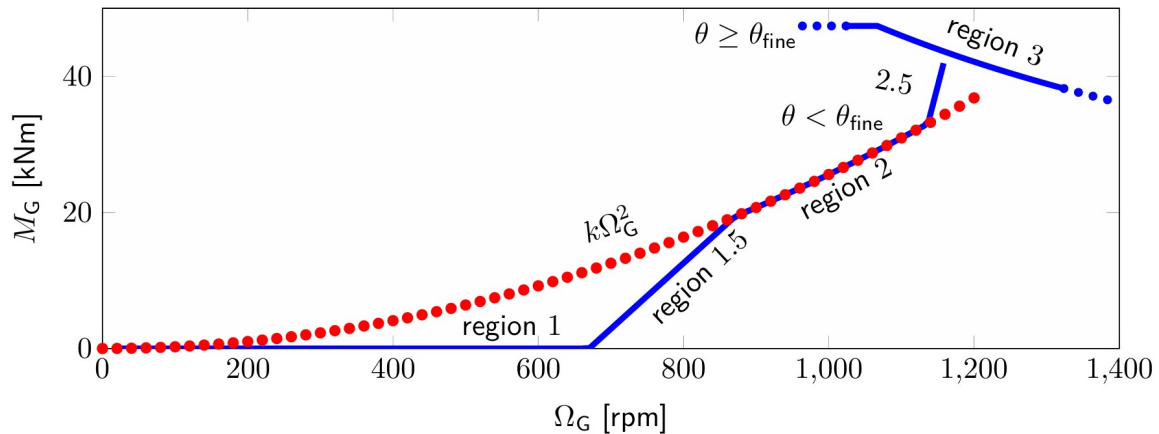


**Figure 2.3** Wind turbine control regions  
[4]

Strategy for the Advanced Torque Controller:

**Region 1.5:** Lowest generator speed  $\Omega_{G,1.5}$  to avoid the 3P frequency interacting with the tower's eigen frequency. Torque PI controller used for fine-tuning.

**Region 2.5:** Generator speed  $\Omega_{G,2.5} = \Omega_{G,rated}$ . Switch from  $\Omega_{G,1.5}$  to  $\Omega_{G,2.5}$  if the measured generator speed  $\Omega_G$  exceeds

$$\Omega_{G,R2switch} = \frac{1}{2}(\Omega_{G,1.5} + \Omega_{G,2.5}) \quad (2.3)$$



Torque Limits:

The generator torque limits are determined by the measured generator speed  $\Omega_G$  and incorporate Anti-Windup mechanisms.

- if  $\Omega_G < \Omega_{G,R2switch}$ :

$$M_{G,lb} = 0 \quad (2.4)$$

$$M_{G,ub} = k\Omega_G^2 \quad (2.5)$$

- if  $\Omega_G > \Omega_{G,R2switch}$ :

$$M_{G,lb} = k\Omega_G^2 \quad (2.6)$$

$$M_{G,ub} = \min \left( M_{G,rated} \frac{\Omega_{G,rated}}{\Omega_G}, M_{G,max} \right) \quad (2.7)$$

**Region 2:** The controller aims to maximize energy yield while ensuring the turbine operates efficiently.

**Region 3:** The torque controller maintains the generator torque at the rated value to protect the turbine from excessive mechanical stress due to high wind speeds.

## 2.4 Collective Pitch Controller (CPC) (Julius)

Collective Pitch Control (CPC) adjusts the pitch for all 3 blades similarly. The pitch control behavior has a high impact on the structural loads therefor on the life time of the wind turbine and thus on costs. CPC can be implemented with a standard PI-Controller. Main task of the CPC is to make the rotor area more permeable for the wind in order to reduce the power coefficient. This is done by pitching the rotor blades in a less advantageous aerodynamic position. With increasing wind speed the power output increases as well as the loads. In order to keep the loads within an acceptable limit the power output of the wind turbine must be limited.

The pitch controller is only active in region 3, when the wind speed is above the rated wind speed as described in figure 2.2. In region 3 the pitch controller maintains rated speed and the generator torque controller rated torque. In the OPTIMUS Shakti wind turbine a gain scheduled PI controller is used to control the rotor speed.

The concept of gain scheduling is widely used and a common feature in blade pitch controllers. With the use of gain scheduling the gain parameter  $kp$  of the controller is changed based on the operating point of the system. The parameter  $\theta_k$  is used to change the gain of the CPC. The operating point is determined by the pitch angle  $\theta$  and based on it with 2.8 the scheduled gain  $kp_{gs}$  is derived.

$$\frac{kp}{\frac{\theta - \theta_{min}}{\theta_k} + 1} = kp_{gs} \quad (2.8)$$

## 2.5 Tower Damper (Felix)

This section describes the the function and the implementation of a pitch angle based Tower Damper (TD). !!! Abbreviation package !!! The design follows the description in [2] similar as the workflow in the exercise of the corresponding lecture and lecture notes [4]. The tower dynamics are modeled as in [2] (eq: 8.12 and 8.13). Here referd as 2.9 and 2.10.

$$M\ddot{x} + D\dot{x} + Kx = F + \Delta F \quad (2.9)$$

$$\begin{aligned} \Delta F &= \frac{\partial F}{\partial \theta} \Delta \theta = -D_{TD} \dot{x} \\ \Delta \theta &= \frac{-D_{TD}}{\partial F / \partial \theta} \dot{x} \end{aligned} \quad (2.10)$$

As described by equation 2.9 the dynamics of the tower in fore-aft direction are lightly damped if  $D$  is small and the force  $\Delta F$  which is the additional thrust force resulting of a pitch action is equal to zero. The force  $F$  is damped by the relative wind speed  $v_{rel} = v_0 - \dot{x}$  and therefore  $F = F(\Omega, \theta, v_{rel})$  [4]. To damp the tower top speed  $\dot{x}$  even further [2] proposes an update of the pitch angle of  $\Delta \theta$ . This will damp the tower motion further as described in 2.10. This lead to a reduction of the tower bottom bending moment. Nevertheless this comes at a cost of higher pitch activity and the damping is only available in control region 3. The static tower top deflection over the regions are shown in section 4.1. This is helpful to see when the damper is active and what can be damped.

The implementation and test of the damper is done in Matlab and Simulink. As in the lecture and the corresponding exercise [4] the tower top acceleration  $\ddot{x}$  is measured in reality. To make the simulation task as similar to a real world application here also the the tower top acceleration is used. What is also taken into account is the existence of a real pitch actuator. This means that the pitch update  $\Delta \theta$  can not be applied instantaneously because of the time constants of the pitch actuator. To address this phenomena there are 2 methods tested. First a direct integration 2.11:

$$\dot{x}(t) = \int \ddot{x}(t) dt \quad (2.11)$$

And second a phase shift of  $90^\circ$  of the speed signal by a Lag-Compensator. The Transferfunction in the frequency domain is shown in equation 2.12. Where the input in the frequency domain is  $\ddot{X}$  and the output is  $\dot{X}$ .

$$\frac{\ddot{X}(s)}{\dot{X}(s)} = \frac{s + z}{s + p} \quad (2.12)$$

$$\dot{x}(t) = \ddot{x}(t) - \int p\dot{x}(t) - z\ddot{x}(t) dt \quad (2.13)$$

The implementation in Simulink is first following the approach in the exercise [4]. The input  $\Omega_{g\_g}$  is already a filtered value. It is low pass filtered and the 3P blade passing frequency is notched. As shown in figure 2.4 to activate the TD the generator power is used. The *LowPassOrder1* is used to reduce the switching frequency of the TD to ensure that it is not switched on and of if the WT is operating near rated conditions. In the activation the gain is

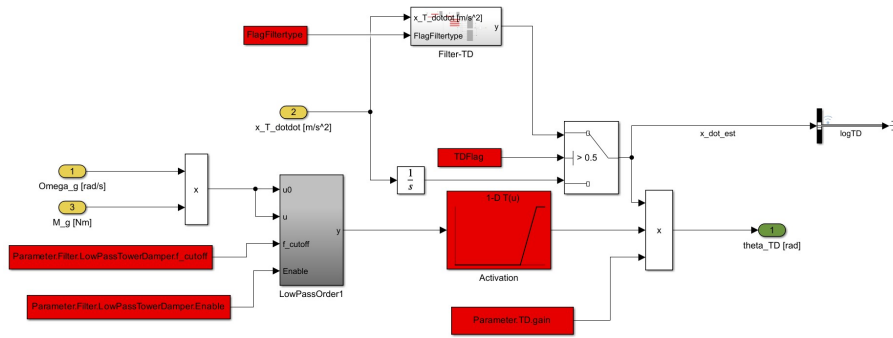


**Figure 2.4** Tower Damper in Simulink model

slowly ramped up from 0 % to 100 % over a power range from 80 % of the rated power to 100 % and stays there.

In the first method, here named integrator, the tower top acceleration signal is integrated and then multiplied with the damping gain *Parameter.TD.gain* and the activation signal as shown in figure 2.4. The resulting quantity is the pitch offset mentioned in equation 2.10. This offset  $\Delta\theta$  is added to the pitchangle control value of the collective-pitch-controller and this together is the new input for the pitch actuator of the SLOW-model.

The second method, here named Lag-Compensator, isolates the tower eigenfrequency by passing the acceleration signal first through a low pass filter and then a high pass filter. The cutoff frequency of the low pass filter is above the eigenfrequency of the tower and the cutoff frequency of the high pass filter is below the eigenfrequency. Now the signal contains mainly the isolated eigenfrequency of the tower with which the tower is oscillating in the fore-aft direction. To phase shift the signal a lag compensator is used. As shown in figure 2.5 the frequency that

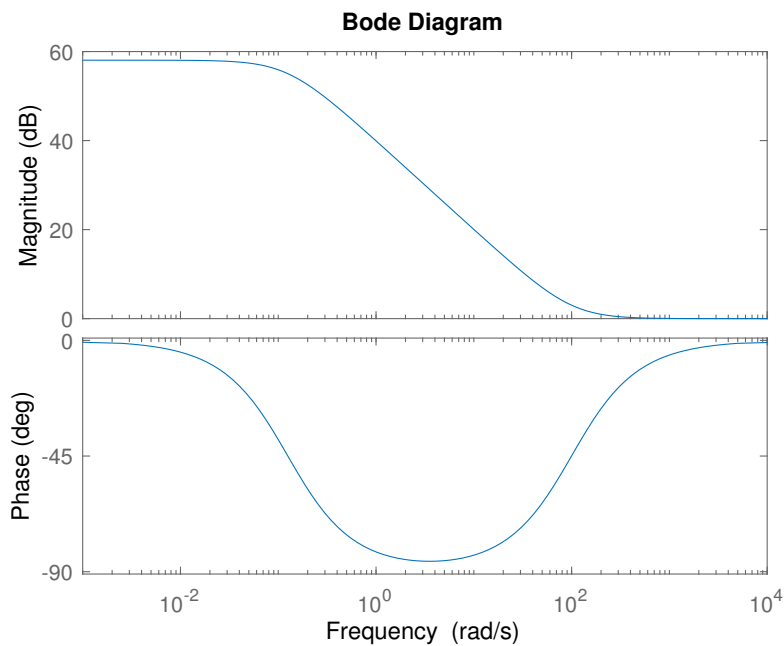


**Figure 2.5** Bode plot of the Lag-Compensator

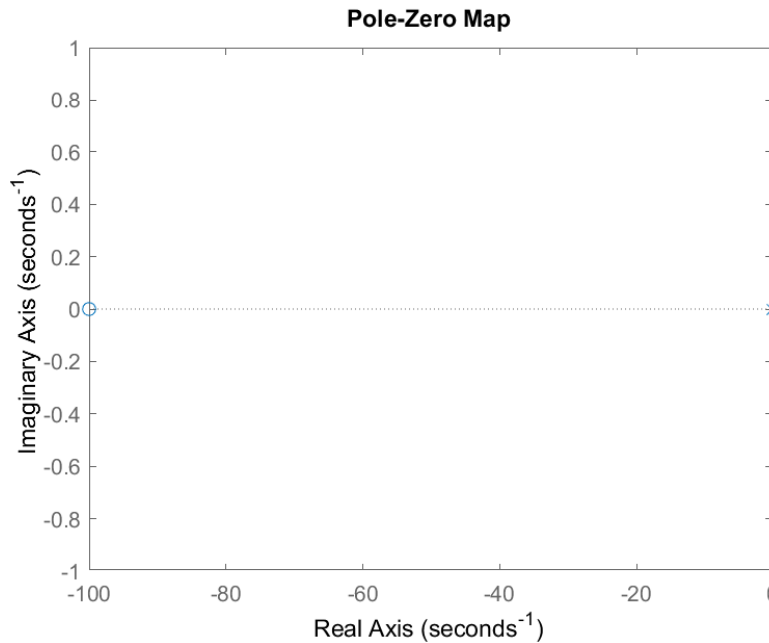


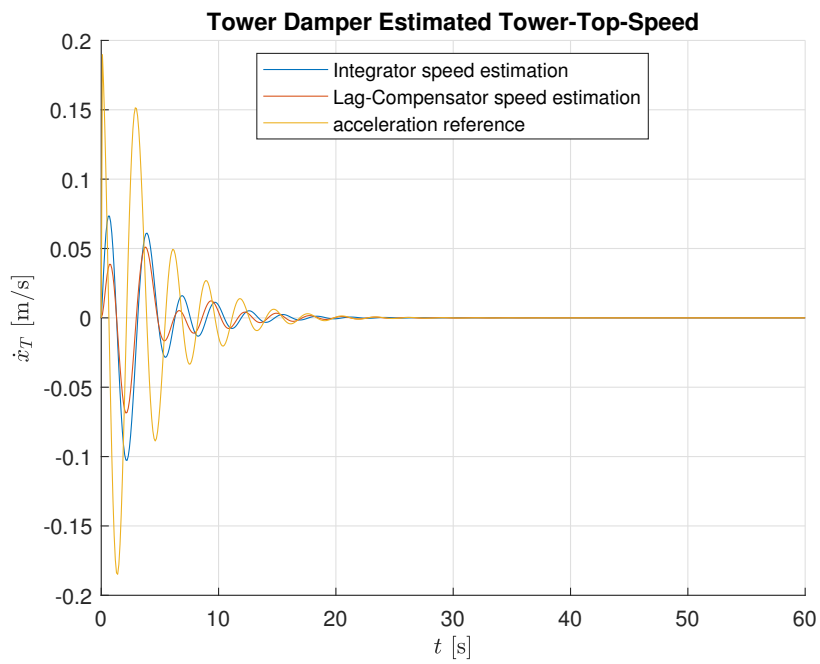
**Figure 2.6** Pole-Zero-Map of the Lag-Compensator

has been isolated by the previous filters is phase shifted by nearly  $90^\circ$  and the magnitude of this frequency is increasing by 30 dB. The increase in magnitude and the general difference in magnitude of the  $\ddot{x}(t)$  signal compared to the  $\dot{x}(t)$  can be achieved by a different gain value which will result in a similar damping behavior. Figure 2.6 shows the Pole-Zero-Map of the Lag-Compensator. The  $\circ$  shows the zero and the  $\times$  shows the pole. the zero  $z = -100$  and the pole  $p = -0.125$  in the shown plot.

The design is tested first with a wind step from  $v_0 = 20 \text{ m/s}$  to  $v_1 = 21 \text{ m/s}$  to ensure the general functionality of the methods shown in figure 2.7. The figure shows the acceleration reference value, both speed estimation methods need to be  $90^\circ$  phase shifted compared to this signal. The figure shows the estimated speeds after the integrator or the *Filter-TD* (see figure 2.4). The displayed values of the Lag-Compensator speed estimation is decreased by a scaling factor  $a = 0.01$  to ensure a comparison in one plot. The plot shows that the speed decays slightly faster with the Integrator method. Due to the different gains of the two methods the scaling factor  $a$  is not needed in figure 2.8, where the tower top speed of the SLOW-model is computed.

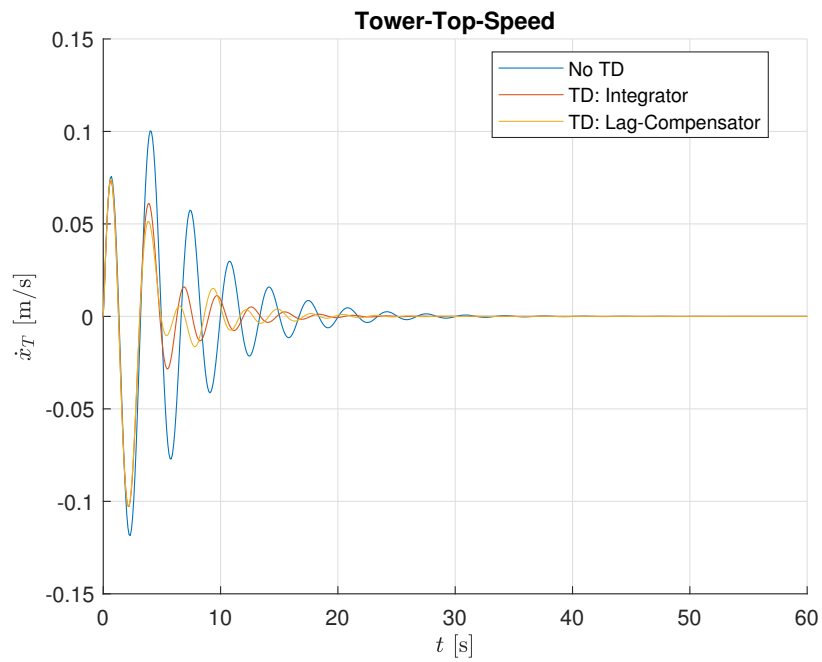
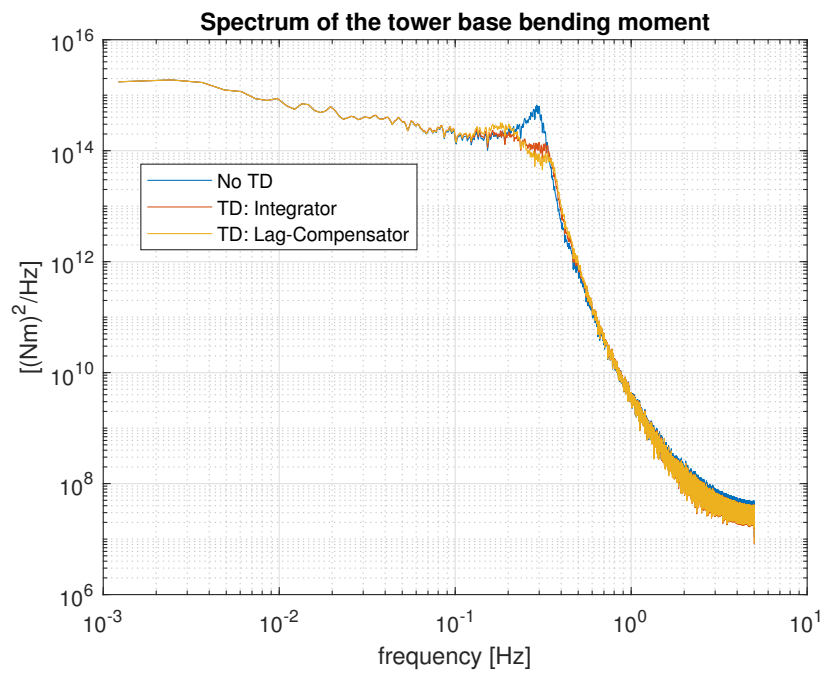
Both methods resulting into a damping of the tower top speed. Nevertheless the integrator method gives better result in the wind step test due to the smother damping of the oscillation. The Lag-Compensator method leads first to a faster damping but to stop the tower movement both methods are nearly equally fast.

To further test them the SLOW-Model is disturbed with a turbulent wind field similar to the exercise in [4]. The reduction in DEL for the tower base bending moment is evaluated by tower base bending moment spectrum computed in figure 2.9. This also shows that both methods reducing the loads at the eigenfrequency of the tower. The comparison of the damping method shows, that the Lag-Compensator has a higher damping effect at the eigenfrequency but leads to higher loads between 0.1 Hz and 0.2 Hz as well as above the eigenfrequency between



**Figure 2.7** Tower Damper Estimated Tower-Top-Speed

0.35 Hz and 0.55 Hz. The Lag-Compensator can be tuned in such a way that the damping at the eigenfrequency is similar to the integrator method which will reduce the loads in the above mentioned frequency ranges.

**Figure 2.8** Tower-Top-Speed**Figure 2.9** Spectrum of the tower base bending moment

### 3 Further Things

#### 3.1 Wind Field Generation (Felix)

To test the turbine model in Simulink with a reasonable disturbance a turbulent wind field has been created. This was done based on [1] and the exercise to lecture 06 of the Master Course "Controller Design for Wind Turbines and Wind Farms".

The used method was to use the IEC Kaimal Spectral Model [1] where the Auto-spectrum of the rotor effective wind speed  $v_0$  is calculated according to equation 3.1.

$$S_{RR} = \frac{S_{ii,u}}{n^2} \sum_{i=1}^n \sum_{j=1}^n \gamma_{ij,u} \quad (3.1)$$

The time series of the wind speed is calculated with the following simulation parameters: including total simulation time  $T$ , time step  $\Delta t$ , random seed for reproducibility, and reference wind speed  $U_{\text{Ref}}$ . The frequency range is determined based on the total simulation time and time step:

$$\begin{aligned} f_{\min} &= \frac{1}{T}, \\ f_{\max} &= \frac{1}{2\Delta t}, \\ \Delta f &= f_{\min}, \\ f &= \{f_{\min}, f_{\min} + \Delta f, \dots, f_{\max}\}. \end{aligned}$$

With the Auto-spectrum according to equation 3.1 the amplitude  $A(f)$  for each frequency component is calculated in equation 3.2.

$$A(f) = \sqrt{2S_{RR}(f)\Delta f} \quad (3.2)$$

Random phase angles  $\Phi$  are generated for each frequency component using a uniform distribution in the range  $[0, 2\pi]$ . The inverse Fourier transform is used to generate the time series as shown in equation 3.3.

$$\begin{aligned} t &= \{0, \Delta t, 2\Delta t, \dots, T - \Delta t\}, \\ U(f) &= \begin{cases} 0 & \text{(DC component),} \\ A(f)e^{i\Phi} & \text{(frequency components).} \end{cases} \\ v_0(t) &= U_{\text{Ref}} + \mathcal{F}^{-1}(U(f)). \end{aligned} \quad (3.3)$$

This is done for the Rotor-area and for a duration of  $T = 3600\text{ s}$  for different reference mean wind speeds  $U_{\text{Ref}}$ . To allow the storage team reasonable simulations on a timescale of several hours or days these time series are combined after a pattern of one hour mean wind speeds as input values. The corresponding turbulent wind series are then selected and combined by circular shifting the time series until the beginning of the new series is matching the end of the previous one to avoid bigger jumps in the wind than expected by the turbulence itself. To achieve this an algorithm is looking in the next time series for values that are near to the end of the old series within a threshold and a number of consecutive numbers to ensure the gradient of next series is not too steep.

One example of a combined turbulent time series is shown in figure 3.1.

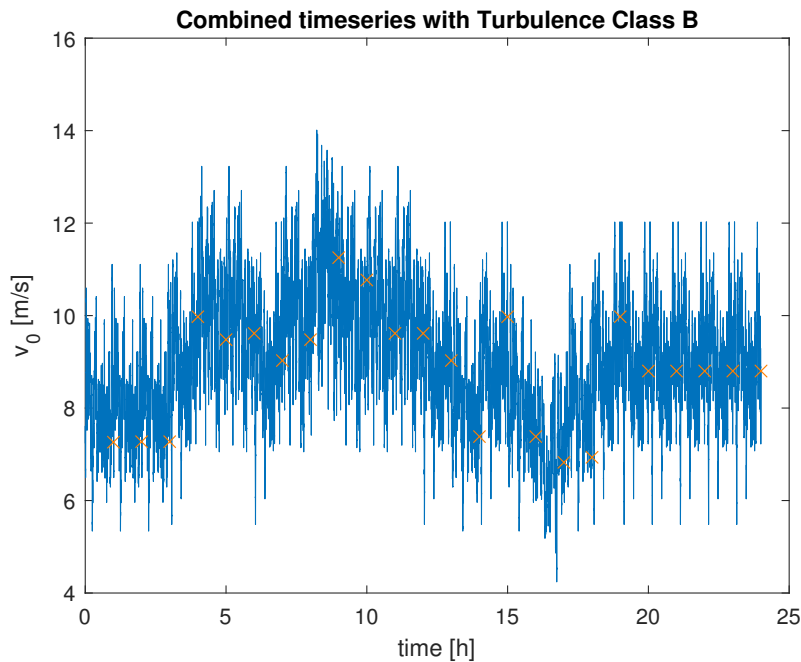


**Figure 3.1** Combined timeseries with Turbulence Class B

## 3.2 Simple Storage System Dummy (Julius)

In order to assist the storage development team in the beginning of the project phase a simple energy storage system dummy was developed and integrated into the used IEA Wind Task 37 3.4 MW reference wind turbine Simulink model (figure 3.2). The further development of the storage model was executed by the storage team.

### 3.2.1 Description

The storage system dummy was realized by a simple battery management system (BMS) in combination with a integrator block. The BMS is capable to simulate the storage in 3 states *standby*, *charge* and *discharge*.



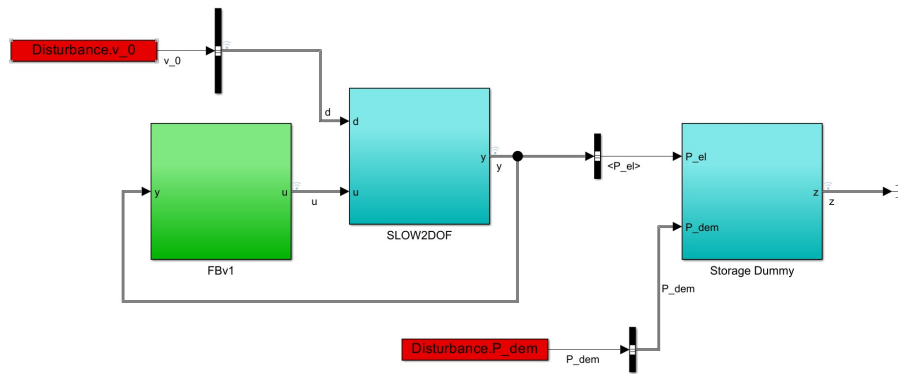


Figure 3.2 Storage dummy in Simulink model

### 3.2.2 Scenarios

In order to explore different possibilities in which the storage system could be applied multiple scenarios where implemented into the simulation model. A curtailment event as described in scenario 5 is shown in figure 3.3.

1. **No grid power demand:** The storage system is in working condition. The storage system is not at full capacity. There is no power in feed into the grid. The storage is getting charged.
2. **Rated power demand from grid:** The storage system is in working condition. There is rated power feed into the grid. The storage is not getting charged.
3. **50 % of rated power demand from grid:** The storage system is in working condition. The storage system is not at full capacity. There is a power demand from the grid of 50 % of rated power. The storage is getting charged with a reduced rate of charge.
4. **Turbine operated below rated power, grid demand is exceeding production:** The storage system is in working condition. The storage is charged to 50 % of its maximum capacity. The WT is operating below rated power and the grid demand is higher than the power production of the WT. The storage system is getting discharged.
5. **Curtailment scenario of 4h in 25h period:** The storage system is in working condition. The storage system is not at full capacity. The WT is operating at rated power. The power must be reduced for a certain amount of time because of a curtailment order from the grid operator. The storage system is getting charged.

### 3.3 Tower Bending Stiffness (Julius)

For the implementation of the tower damper in the SLOW model the tower equivalent bending stiffness  $k_{Te}$  and the initial tower top deflection  $X_{T0}$  is needed. With OpenFAST the steady states calculations (section 4.1) with a wind speed range from 3 m/s to 9 m/s where done. The bending

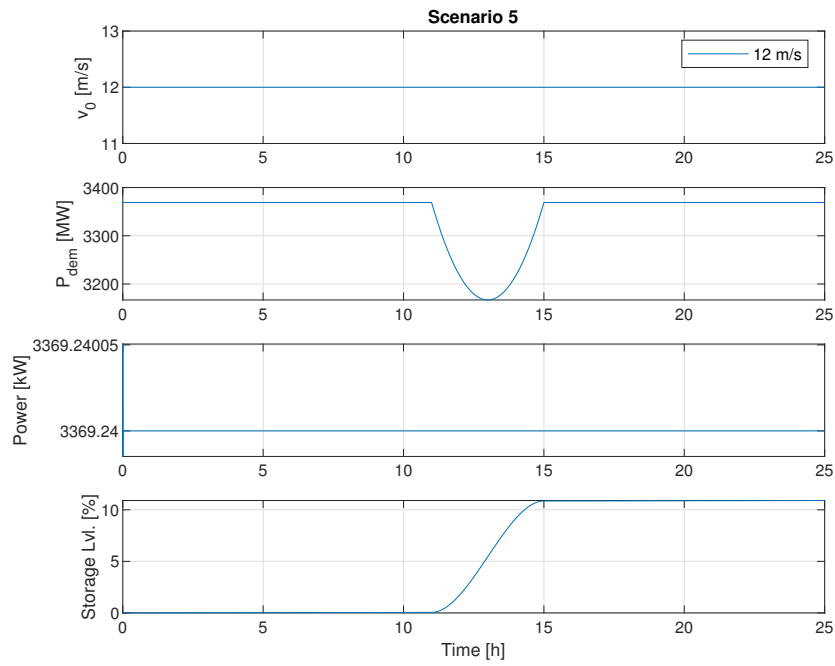


**Figure 3.3** Curtailment scenario for 4h duration, a storage capacity of 5 MWh and a curtailment rate of 6%.

stiffness of the tower can be calculated with:

$$k_{Te} = \frac{F_a}{X_T - X_{T0}} \quad (3.4)$$

Where  $F_a$  is the aerodynamic thrust force onto the rotor plane and  $X_T$  the deflection of the tower top. The initial tower top deflection  $X_{T0}$  is determined from the calculated steady states via a polyfit of the curve to get the deflection of the tower at  $F_a = 0$  N. With 3.4 the bending stiffness in every steady state is determined and averaged over the number of points. This leads to an tower equivalent bending stiffness of  $k_{Te} = 2.185$  MN/m and a initial tower top deflection of  $X_{T0} = -0.021$  m.

## 4 Controller tuning

### 4.1 Steady States (Soni)

The steady states are influenced by the design of the controller and turbine in the simulation. These states are useful for initializing the simulation, as they provide essential information for analyzing the turbine's power behavior and the controller settings. Additionally, these steady states play a crucial role in the overall wind turbine design and can be utilized to initialize further simulations.

The general procedure we followed to find the steady-state parameters is as follows:

- First, find the rated wind speed.
- Then, calculate the steady states below the rated wind speed separately for regions 1, 1.5, 2, and 2.5.
- Finally, calculate the steady states above the rated wind speed.

Find the  $v_{rated}$ ,  $v_{1to1.5}$ ,  $v_{1.5to2}$  and  $v_{2to2.5}$  using the minimization problem method, as show in Equation 4.1. Also, use the minimization problem method to find the above-rated wind speed, as shown in the equation 4.2.

$$\min_{v_0} (M_a(v_0, \Omega, \theta) - M_G)^2 \quad (4.1)$$

$$\min_{\theta} (M_a(v_0, \Omega, \theta) - M_G)^2 \quad (4.2)$$

In 5MW Optimus-Shakti simulation model are performed for complete wind bins ranging from 0 to 30 m/s. To determine if the simulation has stabilized, the standard deviation of the tower top displacement is calculated. The values for wind speed, pitch angle, rotor speed, tip speed ratio, generator torque, and the standard deviation of the nacelle acceleration are determined. Additionally, the results are visually assessed through plots. The values found through simulation are  $v_{rated} = 9.3531$ ,  $v_{1to1.5} = 6.0652$ ,  $v_{1.5to2} = 6.0652$  and  $v_{2to2.5} = 8.6631$ . Figure 4.1 demonstrates the model's static behavior by plotting power against wind speed.

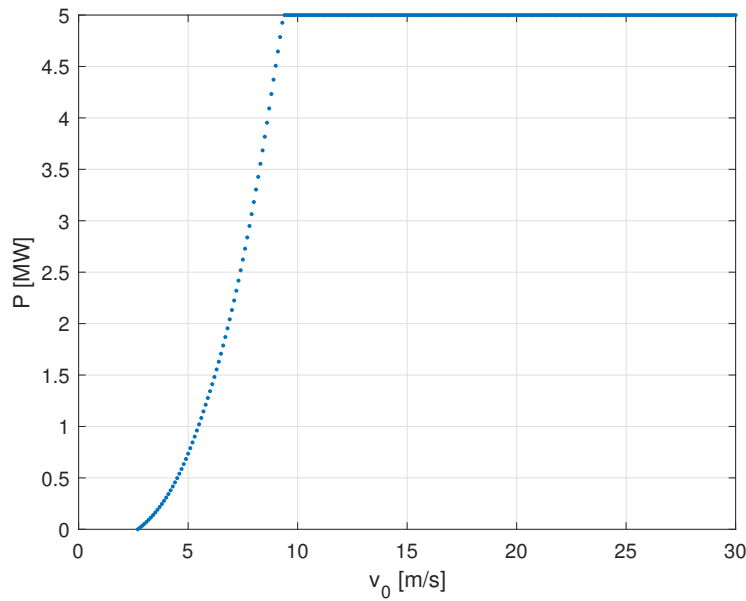


**Figure 4.1** Power curve calculated with steady state calculations

## 4.2 DEL calculations and Parameter Optimization (Felix)

### 4.3 Minimum Pitch Angle Optimization (Julius)

The optimization of the minimum pitch angle is a simple adjustment which leads to a small increase in the AEP. The optimization was done with a brute force approach and the steady states calculations (Section 4.1). In control region 2 the WT should work at optimum  $C_p$  and  $\lambda$ . The use of minimum pitch angle can lead to an more efficient state of the turbine at the start of region 2 and therefor increase the AEP. For different pitch angles the steady states where calculated. As optimum, min. pitch angle the angle which leads to the highest  $C_p$  was chosen. As a result the min. pitch angle of  $0.5^\circ$  was determined and is shown in figure 4.2. During the calculation the pitch angle was optimized in a range of  $0^\circ$  to  $5^\circ$  with a step size of  $0.1^\circ$ .

The determined min. pitch angle of  $0.5^\circ$  leads to an increase in AEP of 0.29 % compared to min. pitch angle of  $0^\circ$ . (Calculated with Weibull parameters of TC III and  $k = 2$ .)

### 4.4 Minimum Pitch Angle Optimization for Control Region 1.5 (Julius)

Since the control region 1.5 has a large wind speed range of 3.28 m/s the optimization of the pitch angle could lead to an increase in AEP. As optimization process a brute force approach was used in order to find the optimum pitch angle for every operating wind speed in region 1.5. During the calculation the pitch angle was optimized in a range of  $0^\circ$  to  $5^\circ$  with a step size of  $0.1^\circ$ . The results of the optimization can be seen in figure 4.3. The result shows, that keeping a static pitch angle through region 1.5 is not leading to the optimal power production. A calculation of the AEP with a dynamic pitch adjustment for region 1.5 leads to an increase of 0.19 % compared to a

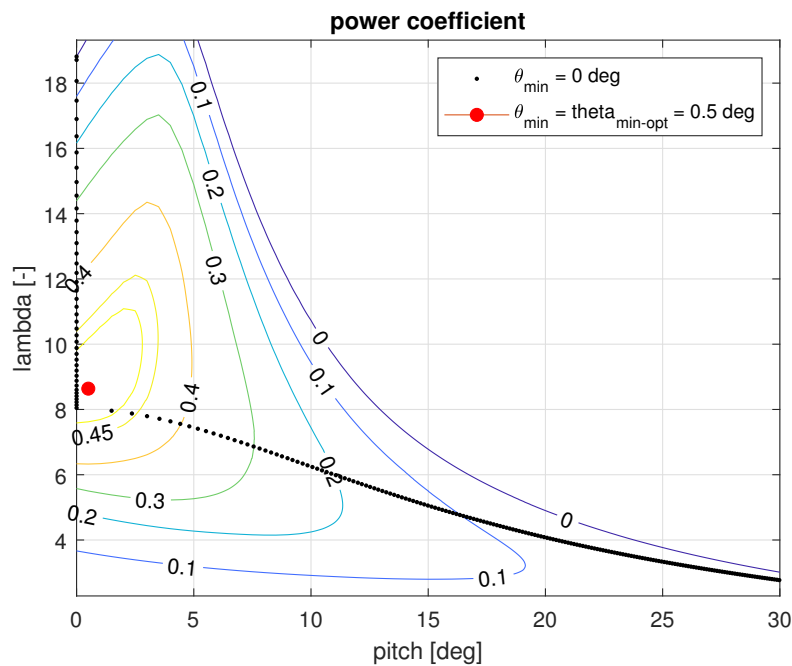


**Figure 4.2** brute force optimization for minimum pitch angle  $\theta$

static minimum pitch angle of  $0.5^\circ$  as shown in section 4.3. (Calculated with Weibull parameters of TC III and  $k = 2$ .) Since the calculation is done without transition regions for the adjustment of the pitch the increase in AEP after implementation of the control behavior is to be expected less than the named 0.19 %. The approach of changing the pitch angle dynamically in region 1.5 was not implemented in the OPTIMUS Shakti project but could be interesting for further optimization of the developed WT.

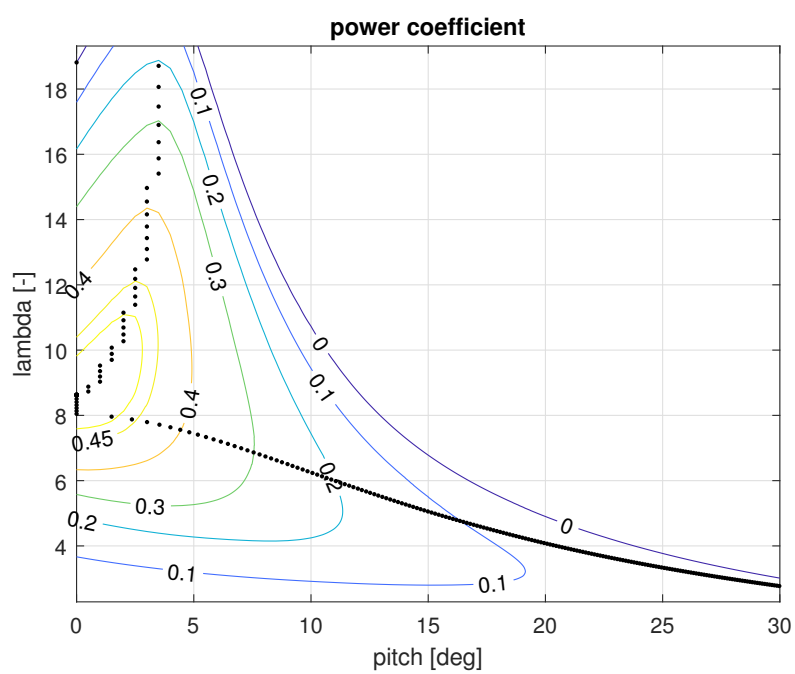


**Figure 4.3** brute force optimization for minimum pitch angle  $\theta$  in region 1.5

## 5 Challenges, Teamwork and Lessons Learned

### 5.1 Rated Wind Speed (Julius)

In order to get started with the project some specifications of the turbine had to be decided really quick. In this particular case the value of the rated wind speed lead to some confusion during the development phase of the Shakti WT. After the rotor blades where aerodynamically designed the steady states calculations revealed a problem with the rated wind speed. It was discovered that the design value of the rated wind speed was not fitting to the aerodynamic behavior of the rotor.

An investigation in cooperation with the project management lead to the result, that the decision regarding the rated wind speed was not based on the same source as rotor diameter, rated power and  $C_p$ . This lead to large mismatch in between the listed values.

The basis for the decision of the rotor diameter based on the fixed value of rated power was done by using a data base of multiple similar turbines with similar technical specifications. From the database a power per square meter value was derived from which the rotor diameter was calculated. The  $C_p$  value and the rated wind speed was calculated based on the scaling of a power curve from a Servion WT.

The unchecked use of the calculated power per square meter value which already contained an unknown averaged  $C_p$  value in combination with the chosen  $C_p$  and rated wind speed from the scaled power curve lead to the mismatch. In absolute numbers the difference where a calculated rated wind speed value of 9.3 m/s compared to the design value of 10.61 m/s.

In order to fix the issue the 4 following options where proposed: The fixed design values at that time where: rated wind speed 10.61 m/s, rotor diameter 178 m, rated power 5 MW,  $C_p$  0.48.

1. Keep rated wind speed and **power**, but **reduce** Rotor radius.  $C_p = 0.48$  for  $R = 140$  m
2. Keep rated wind Speed and **rotor** radius, but **increase** rated power.  $C_p = 0.3$  for  $P = 5.5$  MW
3. Keep rated power and rotor radius and accept new rated wind speed at ca. 9.3 m/s.
4. Keep the design values and use the "peak shaving" method to start pitching already before region 3 in order to only reach rated power at a higher wind speed.

Since the project aim is to build a WT for low wind speed regions in collaboration with the project management and the project owner the decision was made to go with the option number 3 and accept the new rated wind speed.

## 5.2 Generator Speed and Control Region 2.5 (Felix)

In addition to the challenge described in the previous section 5.1 we discovered another one during the first iteration of the Steady States calculation. The rated conditions were met before we get into the Control Region 2.5. The cause of this was the rated generator speed of  $\Omega_{G,\text{rated}} = 458 \text{ rpm}$  was set too high with the aerodynamic efficiency at this time. After we discovered this issue and addressed it with the electrical drive train team, they provided us a new design value (see Steady States 4.1), by increasing the number of poles in the generator. These value changes of rated wind speed 5.1 and the generator speed resulted in a first draft of the Steady States of the Shakti WT as described in 4.1.

The issue isn't fully resolved here because we triggered an infinite design loop here. Hence the mechanical drive train team is not calculating the gearbox ratio  $r_{\text{GB}}$  with the  $\lambda_{\text{opt}} = 8.75$  but with another design value proposed by the management: The tip speed at  $\lambda_{\text{opt}}$ . Which is defined as  $v_{\text{Tip}} = 80 \text{ m/s}$ . So after the changes of the generator speed  $\Omega_{G,\text{rated}}$  a new gearbox ratio  $r_{\text{GB}}$  was calculated this would lead to the same issue described in the paragraph above. After clarification with the management we were able to resolve this issue because the tip speed was a maximal value  $v_{\text{Tip}} = \hat{v}_{\text{Tip}}$ , which we were not allowed to overstep but not a hard design value. The resulting solution is to keep the original gearbox ratio and adjust the Generator speed as described above.

## 5.3 Mismatch of SLOW and FAST Model (Julius)

During development and the release of the first OpenFAST (FAST) version of the WT controller big problem was encountered. In order to validate the new controller version for FAST a simulation was done and the results were compared to the expected behavior of the turbine and the SLOW model of the developed WT. The findings were inconclusive. The simulations carried out showed for the same conditions, such as constant wind, no pitch activity and a matching number of DOFs a difference in power production of 16 %. The FAST model showed for rated wind conditions a 16 % lower power output compared to the SLOW model.

After investigating several possibilities in SLOW and FAST the aerodynamics in FAST were identified as the cause of the mismatch. The rotor blades team provided a  $C_p$  lookup table with the software QBlade which is used by the SLOW model for deriving the correct aerodynamic power from the rotor within the Simulink model. Since FAST was used for the load simulations the blade design in QBlade had to be exported. FAST in this case is not using a  $C_p$  look up table and is instead calculating the aerodynamics directly from the blade design. The design is input via the airfoil data and the corresponding position along the blade. The load simulations in FAST were based on the AerodynV15 module. Because QBlade is only supporting the export up to version AerodynV13 the conversion from AerodynV13 to V15 was done separately by the rotor blades team. During this conversion an unidentified error occurred and led to the faulty aerodynamics which led to a difference in power production.

As a solution the change from the AerodynV15 module to the AerodynV14 module was approached. This was done because the conversion from the QBlade output in AerodynV13 is



compatible with the AerodynV14. The change from one aerodyn version to another revealed that faulty airfoil data was exported by QBlade. The files contained random NaN values as certain key values. This problem was solved by correcting the wrong values after the export. The change from AerodynV15 to AerodynV14 were able to solve the issue and make the SLOW and FAST simulation match.

The faulty exported data was not the cause for the mismatch of AerodynV15. This problem is still unclear.

As in section 5.1 described the rated wind speed was reduced during the design process from 10.61 m/s to 9.3 m/s. Because of the higher wind speed used for the FAST simulations up to that point the low aerodynamic power output was only identified quite late during the design process. With the incorrect rated wind speed the WT was apparently providing the rated power. Which in truth the turbine was operating way above wind conditions to reach rated power. Nevertheless the problem was identified in time and solved as a team effort of the loads, blades and control team. The described issue shows, that the validation of a model is from high importance and mistakes in totally different areas of responsibilities can lead to unexpected behavior later in the development phase.

## 5.4 High Blade Mass and Generator Inertia (Julius)

Generator inertia and blade masses have significant influence on the dynamic behavior of the wind turbine. For the tuning of the controller and updating the used Simplified Low-Order Wind turbine (SLOW) model the exact knowledge of above mentioned values are necessary.

During the project development phase the inertias of the wind turbine were obtained from the OpenFAST (FAST) model. The controller tuning was done with these values and showed in the weekly presentation. During the presentation the dynamic behavior of the turbine was criticized because the turbine took 90 s to recover from a wind step of 7.0 m/s to 7.1 m/s. Investigating the cause lead to the finding that the mass of the rotor blades were not correct in the FAST model. The updated masses from the first rotor blades draft were 17-times higher than the ones before the update. These high masses caused the long reaction time (90 s) of the simulation model. Correcting the masses resolved the described issue and lead to a more realistic reaction time of 30 s.

One update of the generator inertia lead to confusion because the received value was about 45-times higher than before. Checking different references lead to the result, that the given value couldn't be correct. The developed wind turbine is equipped with a 5 MW generator. Similar wind turbines have a inertia of 500 kgm<sup>2</sup>, the first provided value was 24 000 kgm<sup>2</sup>. For comparison a value for the inertia of a 33 MW generator is 2293 kgm<sup>2</sup> [3]. Contacting the responsible departments resolved the issue quickly and lead to the final value of 782.44 kgm<sup>2</sup>.

Both incidents show that a plausibility check of values after receiving and before sending is important to avoid mistakes in presentations. Communication between responsible groups is key to resolving such normal issues quickly and correctly.

## 5.5 Lessons Learned (Julius)

In conclusion all challenges encountered during the development of the Optimus Shakti 5.0 wind turbine were properly resolved. Some key aspects that were learned from solving the described challenges in the section before are the following ones:

- **Model validation** is crucial before releasing the model/information to other participants of the project or working with a given model.
- **Plausibility check** of provided values and results either by comparing with previous or researching similar ones.
- Using **small steps** to apply changes in order to be able to keep an overview what changed in case unexpected behavior occurs.
- **Making the problem smaller** such as deactivating parts of a simulation model that are not necessary in order to isolate the fault. (e.g. the controller or multiple Degree Of Freedom (DOF))

## 5.6 Team (Felix)

## 6 Summary (Felix)

### 6.1 Conclusion

$\pi$  hallo Microsoft (MS)

### 6.2 Improvements and Future Workflow

## 7 Appendix

### 7.1 Project Order (Julius)

### 7.2 Control Parameter (Felix)

### 7.3 Steady States (Julius)

Wind Speed [m/s]	Pitch Angle [deg]	Rotor Speed [rpm]	Power [kW]
3	0.50	5.62	52
4	0.50	5.62	309
5	0.50	5.62	735
6	0.50	5.62	1343
7	0.50	6.49	2132
8	0.50	7.41	3182
9	0.50	8.03	4507
10	4.81	8.03	5000
11	7.81	8.03	5000
12	10.06	8.03	5000
13	12.00	8.03	5000
14	13.71	8.03	5000
15	15.29	8.03	5000
16	16.79	8.03	5000
17	18.21	8.03	5000
18	19.55	8.03	5000
19	20.84	8.03	5000
20	22.09	8.03	5000
21	23.31	8.03	5000
22	24.49	8.03	5000
23	25.64	8.03	5000
24	26.77	8.03	5000
25	27.86	8.03	5000

## References

- [1] I. 61400-1. *Wind turbines - Part 1: Design requirements*. International Electrotechnical Commission, 2005.
- [2] T. Burton, N. Jenkins, D. Sharpe, and E. Bossanyi. *Wind Energy Handbook*. New York, USA: John Wiley a Sons, 2011.
- [3] A. Gloe, P. D. C. Jauch, and T. R  ther. "Grid Support with Wind Turbines: The Case of the 2019 Blackout in Flensburg". In: *Energies* 14.6 (2021), p. 1697. ISSN: 1996-1073. DOI: 10.3390/en14061697. URL: <https://www.mdpi.com/1996-1073/14/6/1697>.
- [4] P. D.-I. D. Schlipf. *Lecture: Controller Design Objective and Modeling*. 2024.